# Synthesis of a Polymer Skeleton at the Inner Leaflet of Liposomal Membranes: Polymerization of Membrane-Adsorbed pH-Sensitive Monomers

Dominic Gutmayer,[†] Ralf Thomann,[‡] Udo Bakowsky,[§] and Rolf Schubert*[,†]

*Lehrstuhl für Pharmazeutische Technologie und Biopharmazie, Albert-Ludwigs-Universität, Hermann-Herder-Strasse 9, D-79104 Freiburg im Breisgau, Freiburger Materialforschungszentrum und Institut für Makromolekulare Chemie, Albert-Ludwigs-Universität, Stefan-Meier-Strasse 21, D-79104 Freiburg im Breisgau, and Institut für Pharmazeutische Technologie, Philipps-Universität, Ketzerbach 63, D-35032 Marburg*

*Received June 23, 2005; Revised Manuscript Received February 2, 2006*

We describe the synthesis of liposomes with an artificial membrane skeleton as a model of the native cellular cytoskeleton. Similar to natural conditions, a flat polymer network is coupled to the inner membrane leaflet like a suspended ceiling via membrane-inserted anchor monomers with a spacer. The polymer is composed of DMAPMA (*N*-(3-*N*,*N*-dimethylaminopropyl) methacrylamide) and TEGDM (tetraethylene glycol dimethacrylate) as a linker and is coupled to the membrane anchor DOGM (1,2-distearyl-3-octaethylene glycol glycerol ether methacrylate). In the first step of the synthesis, DMAPMA and TEGDM are encapsulated into liposomes composed of egg phosphatidylcholine (EPC), and free monomers are removed by gel chromatography. At pH 10, DMAPMA adsorbs to the inner membrane surface, as demonstrated in parallel studies with lipid monolayers using a Langmuir film balance. The polymerization by UV irradiation was initiated with DEAP (2,2-diethoxyacetophenone) as the initiator and was shown to be complete after 15 min. At pH 6, polymer was desorbed from the inner membrane surface to form a lamellar structure similar to that of the cellular cytoskeleton, as shown by electron microscopy. In comparison to NIPAM (*N*-isopropylacrylamide), which was used as a monomer in a recent study (Stauch, O.; Uhlmann, T.; Frohlich, M.; Thomann, R.; El-Badry, M.; Kim, Y.-K.; Schubert, R. *Biomacromolecules* **2002**, *3*, 324−32), DMAPMA shows much slower membrane permeation leading to an essential restriction of the formed polymer to the liposomal interior. The DMAPMA-based composite structure stabilizes the lipid membrane against sodium cholate by a factor of 2.5 as compared to plain EPC liposomes. This is discussed in the context of the situation in the liver, where the cytoskeleton probably plays a crucial role in the stabilization of the membrane against high bile salt concentration.

## Introduction

Liposomes, i.e., artificial phospholipid vesicles, are widely used as carrier systems for the targeting of drugs or proteins to particular tissues via the bloodstream.[1−5] Liposomes can also be used as models of cellular membranes,[6−8] e.g., to measure permeation kinetics[9−11] or the binding of substances.[12,13] Their similarity with cell membranes is due to the self-organization of the phospholipids to form bilayers which have properties almost identical to those of lamellar structures found in natural membranes. However, cellular plasma membranes have a higher mechanical stability and different viscoelasticity compared to vesicles consisting of a similar lipid composition.[14,15] Another fact is that the stability of liposomes against bile salts[16] is much lower than that of plasma membranes at the canalicular site of hepatocytes, where there is a high bile salt concentration of up to 40 mM.[17,18] One possible explanation of this enhanced stability is the cytoskeleton, the membranous part of which consists of a flat hydrophilic protein network at the inner membrane surface linked with anchor proteins in the membrane.[19] Recent studies have entrapped the essential compounds of the natural cytoskeleton into giant vesicles in order to study their structural properties after cross-linking.[20]

A number of other strategies have been developed to stabilize liposomes for use as drug carriers or as model membranes through the use of synthetic polymers in the role of the cytoskeleton. Examples are polymerized lipids,[21−24] coating of liposomes with polymers,[25−27] or polymer scaffolds in the lipid membrane.[28]

Our goal is to mimic the cellular cytoskeleton by a composite structure formed by a shell-like polymer network linked via a hydrophilic spacer to the inner membrane monolayer in liposomes. First, skeleton liposomes of this type have been synthesized by polymerization of *N*-isopropylacrylamide (NIPAM) as a water-soluble monomer with 1,2-distearyl-3-octaethylene glycol gylcerol ether methacrylate (DOGM) as a membrane anchor and tetraethylene glycol dimethacrylate (TEGDM) as a cross-linker.[29] By addition of the radical initiator 2,2-diethoxyacetophenone (DEAP) to the external aqueous space, polymerization takes place predominantly close to the inner membrane surface when the initiator enters the liposome. The polymer skeleton then has a hollow sphere-like structure, as shown by electron microscopy and atomic force microscopy (AFM)[29] or by light scattering.[30] This inner-membrane skeleton has already been shown to protect the bilayer membranes against bile salt concentrations comparable to those found in the liver canaliculi.[29]

A drawback to the use of NIPAM as a skeleton monomer unit is its rapid membrane permeation before the polymerization reaction. The permeation rate on a time scale of seconds makes

* To whom correspondence may be addressed. Tel (+49) 761 203 6336; fax (+49) 761 203 6366; e-mail rolf.schubert@pharmazie.uni-freiburg.de.

[†] Lehrstuhl für Pharmazeutische Technologie und Biopharmazie, Albert-Ludwigs-Universität.

[‡] Freiburger Materialforschungszentrum und Institut für Makromolekulare Chemie, Albert-Ludwigs-Universität.

[§] Philipps-Universität.

10.1021/bm0580126 CCC: $33.50 
Published on Web 03/28/2006

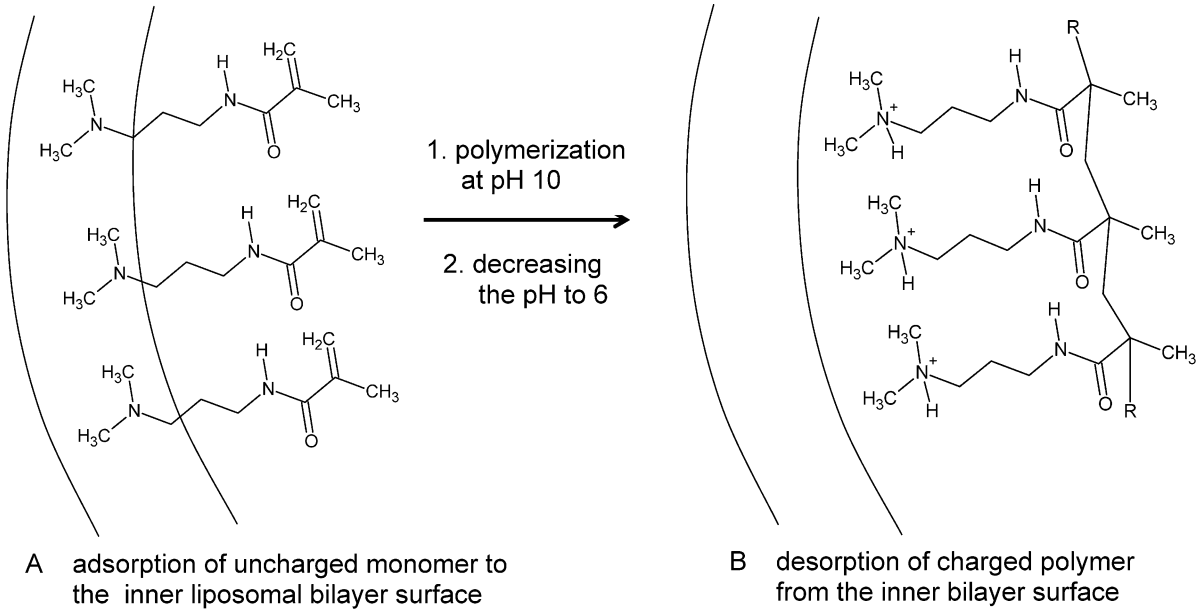


**Figure 1.** Schematic representation of the polymer synthesis at the inner liposomal membrane surface. (A) The weakly basic monomer DMAPMA adsorbs at pH 10 with its uncharged lipophilic part to the inner lipophilic part of the membrane bilayer and is then polymerized together with a membrane anchor and a linker at the membrane surface. (B) After polymerization, the pH is decreased to 6, and the charged and hydrophilic laminar polymer is desorbed from the membrane surface.

a polymerization of exclusively encapsulated monomer impossible. Liposomes were therefore prepared by detergent removal, resulting in equilibrium of NIPAM inside and outside the liposomes. After polymerization, polymers are therefore also found in the external space in addition to the inner skeleton.

In this study, we introduce an enhanced concept for the synthesis of membrane-skeleton liposomes (MSL). *N*-(3-*N*,*N*-dimethylaminopropyl) methacrylamide (DMAPMA), as a slow membrane-permeating monomer, is encapsulated into liposomes by detergent removal, which ensures high encapsulation efficiency and unilamellarity of liposomes.[31] The nonencapsulated portion is removed by size exclusion chromatography. At a pH above the p$K_a$ value of 9.25, the monomer as a weak base is sufficiently lipophilic to be attached to the inner membrane surface, and is therefore polymerized together with a linker and the membrane anchor to form a laminar hollow-sphere structure. After adjusting the pH to 6, the polymer is then detached to form a structure like a suspended ceiling, i.e., the flat polymer layer is still connected with the membrane via the PEG moiety of the anchor molecule functioning as a hydrophilic spacer (see Figure 1). Furthermore, essentially no polymer is formed in the external space outside of the liposomes.

## Experimental Section

**Materials and Methods.** *Compounds for Vesicle Preparation.* Egg yolk phosphatidylcholine (EPC, >98% phosphatidylcholine) was a generous gift from Lipoid (Ludwigshafen, Germany). Radioactive dipalmitoyl phosphatidyl choline ($^{14}$C-DPPC) was purchased from DuPont NEN (Bad Homburg, Germany). The reactive membrane anchor 1,2-distearyl-3-octaethylene glycol glycerol ether methacrylate (DOGM) was synthesized as described earlier.[29] *N*-(3-*N*,*N*-dimethyl aminopropyl) methacrylamide (DMAPMA, Roehm, Darmstadt, Germany) was used as a monomer, tetraethylene glycol dimethacrylate (TEGDM, Röhm, Germany) as the cross-linking agent, 2,2-diethoxyacetophenone (DEAP) as the initiator (Sigma, St. Louis, MO), and methoxyphenol as the polymerization inhibitor (Merck, Darmstadt, Germany). The detergent *n*-octyl-*β*-D-glucopyranoside (OG) (Fluka, Switzerland) was used for the formation of mixed micelles, and Amerlite XAD 1180 Biobeads (a generous gift from Rohm & Haas, Chauny, France) were used as a resin for liposome preparation by detergent removal.

*Monomer Lipophilicity at Different pH Values.* The octanol/water distribution coefficient log *D* of DMAPMA was determined at 25 °C using a semiautomatic titration device (PCA 200, Sirius, Forrest Row, U.K.).

This method is based on a two-phase potentiometric titration approach, by which DMAPMA is titrated in the presence of octanol. As a function of the lipophilic solvent, the p$K_a$ value is shifted, and this shift and the phase ratio volume are used to calculate the distribution coefficient. The distribution coefficient is defined as the ratio of the concentrations of charged and uncharged molecule species in the octanol and the aqueous phase.

First, 10−20 mg DMAPMA were dissolved in water containing 150 mM KCl; the solution was then preacidified to pH 1.8−2.0 with 0.5 M HCl and then titrated alkalimetrically to pH 11.5. A first aqueous titration was performed in the range between pH 5 and 11.5. Next, the experiment was repeated in the presence of different amounts of octanol and the lipophilicity profile log *D*/pH was calculated (Software Control 200 V1.0 and Refine 200; Sirius).

*Studies of pH-Dependent Monomer Adsorption to Monolayers.* The monolayer investigations were carried out using a commercial film balance (RK1, R&K GmbH, Mainz, Germany) with a rectangular thermostated Teflon trough (dimensions 34 mm × 297 mm, 3-mm depth). The surface pressure was measured by a filter paper Wilhelmy balance (BT 01-M, Optrel, Berlin, Germany). For the film balance experiments, the lipid EPC was dissolved in chloroform, in which 100 μL chloroform solution containing 25 μg EPC was spread to the ultrapure water surface (subphase: 45 mL of particle free water, 18.2 MΩ, Millipore Simplicity 185, Eschborn, Germany). After spreading, the lipid films were equilibrated to zero surface pressure for 10 min before the measurements were started. All films were dynamically compressed with a constant speed of 0.15 cm$^2$/s (2.5 × 10$^{-3}$ nm$^2$/s per molecule). All experiments were performed at 25 °C.

After compression of the lipid monofilm to 15mN/m (0.7 nm$^2$/molecule), the film was equilibrated for 60 min to a constant film area. At this point, 1 mL of the subphase was removed with a syringe, and 1 mL of an aqueous monomer solution with the appropriate pH was homogeneously injected into the subphase behind the barriers. After injection, the total monomer concentration reached a value of 4.0 mM. The increase of the surface area dependent on monomer adsorption was recorded under constant pressure conditions for 120 min. For

measuring monomer adsorption, the subphase consisted of water adjusted to pH 6.0 or 10.0 with HCl or NaOH.

*Detergent Removal from Mixed Micelle Solution.* For the rapid preparation of monomer-containing liposomes, the method of detergent removal from mixed micelles by adsorption to divinylbenzene polymer beads[32] (BioBeads Amberlite XAD 1180) was modified. First, the adsorption kinetics of compound to the beads was determined and the optimum parameters were then used to prepare liposomes encapsulating reactive monomer for further polymerization. For this purpose, anchor monomer and detergent were dissolved in chloroform in a round-bottom flask lipid, and solvent was removed by rotary evaporation at 30 °C. In the case of preparation of radioactive polymer liposomes, 50 kBq (1.5 $\mu$Ci) $^{14}$C-DPPC were added to the chloroform solution. Two milliliters of borate buffer (5 mM boric acid, pH adjusted to 10.0 with NaOH) were added to the dry film along with the water-soluble monomers to yield a mixed micelle solution containing 125 mM OG (detergent), 25 mM EPC (lipid), 0.5 mM DOGM (reactive anchor), 160 mM DMAPMA (monomer), and 8 mM TEGDM (linker). Resin beads were washed and purified[33] and stored in demineralized water. Before use, the excess of water was removed from the beads by the use of a suction filter. Two grams of the beads were added to the mixed micellar solution in a glass tube. Residual water in the pretreated beads caused an initial dilution of the solution down to approximately 15−20 mM lipid. The suspension was slowly rotated (250 upM for 15 min) to ensure continuous mixing of the beads with the solution.

*Adsorption Kinetics of Compounds to BioBeads.* After different time points of incubation of the mixture, 70 $\mu$L samples were drawn, and beads were removed by centrifuging (30 s, 500 × g) through 5 mL empty bond elute columns (Varian, Darmstadt, Germany). The concentrations of OG, DMAPMA, and EPC in the centrifugates were determined by high-performance thin-layer chromatography (HPTLC). For each compound to be analyzed, samples and calibrators were pipetted on HPTLC plates (silica gel 60 $F_{254}$, Merck, Darmstadt, Germany), and plates were developed in ethyl acetate/methanol/25% ammonia (50:50:1 vol). For the analysis of OG, after development and drying, the plate was shortly placed in methanol/acetic acid/sulfuric acid anise aldehyde (170:20:16:1 per vol) and dried for 10 min at 105 °C. Deep blue spots were quantified by laser densitometry (TLC scanner 3, Wincats software 1.2.3, Camag, Muttenz, Switzerland). DMAPMA- and EPC-containing spots were quantified by the densitometer at 200 nm without further staining after total drying of the plates.

*Optimized Liposome Preparation.* Liposome formation from mixed micelles using Biobeads occurred within a few minutes, indicated by opalescence of the supernatant of the dispersion. The total processing time was 15 min in order to ensure complete removal of the detergent. In the last 5 min, the pressure was reduced to 100 mbar to remove dissolved oxygen. The mixture was then poured into 5 mL empty Bondelute columns under a nitrogen atmosphere to remove the beads by centrifugation (30 s, 500 × g), yielding 1.5−1.8 mL of liposome dispersion, which was stored under nitrogen atmosphere until further use.

*Removal of Nonentrapped Monomers from Liposomes.* Five-milliliter bond elute columns were filled with a degassed suspension of Sephadex G-50 fine (Pharmacia Biotech, Sweden) in borate buffer pH 10 under nitrogen, centrifuged for 5 s at 50 × g, filled again to the top with the suspension, and centrifuged again for 40 s at 50 × g to remove any excess buffer. Then, each 150 $\mu$L of the liposome dispersion were put on the top of a gel-filled column, which was then immediately centrifuged for 30 s at 500 × g. Free monomer was initially essentially absent in the centrifugates. Their volume was approximately 1.5 mL, and the recovered amount of applied liposomes was approximately 30%, yielding a lipid concentration of around 0.6 mM. Centrifugates were collected under nitrogen for further use.

*Release Kinetics of Liposomally Entrapped Monomer.* At different time points after removal of free monomer, each 150 $\mu$L of the collected centrifugates were put to fresh gel-filled columns and centrifuged for 30 s at 500 × g. For analysis of liposome-encapsulated monomer, centrifugates were analyzed by HPTLC as shown above. Samples were analyzed either immediately or after storage at −26 °C. Monomer relase kinetics was measured from liposomes with or without reactive membrane anchor and from liposomes prepared in 5 mM borate buffer pH 6.0, 9.0, or 10.0.

*Synthesis of Membrane Skeleton by Photopolymerization.* For polymerization, 1.5−2 mL of liposomes were pipetted into a nitrogen-flushed quartz tube containing a magnetic stir bar immediately after removal of free monomer by gel centrifugation, and 1 $\mu$L of the initiator DEAP was added under stirring. Polymerization was then performed by exposure to a UV lamp (2 × 15 W, 254 nm) at a distance of 2 cm for 15 min.

*Polymerization Kinetics.* At various time points during polymerization, 150 $\mu$L liposome samples were mixed with 150 $\mu$L of buffer containing 0.5 mg 4-methoxyphenole (polymerization inhibitor), and the decreasing amount of reactive monomer was analyzed by HPTLC.

*Characterization of Liposomes.* The size of the liposomes was determined by photon correlation spectroscopy (Zetamaster, Malvern Instruments, Herrenberg, Germany). Samples were diluted with either particle-free filtered water or buffer, respectively, to get an optimum scattering intensity of 50−200 kcounts/s. Z-average of the hydrodynamic radius and polydispersity index was determined at 25 °C. The lipid concentration of the liposomal dispersions was determined by their phosphorus content.[34]

*Stability of Liposomes against Sodium Cholate.* $^{14}$C-labeled liposomes were used for the quantification of membrane solubilization by sodium cholate. In 4-mL thick-walled polycarbonate tubes, 940 $\mu$L solutions of sodium cholate up to a concentration of 30 mM in sodium borate buffer at pH 6 were mixed with 60 $\mu$L of radioactive polymer liposomes or EPC liposomes with 2 mol % DOGM (membrane anchor monomer). Total lipid concentration was 1.0 mM. After 15 min of incubation, samples were centrifuged at 20 °C, 95 000 × g for 3 h (ultracentrifuge Optima LE-80, rotor Ti 50.4, Beckman Instruments, Munich, Germany). 200 $\mu$L of the supernatants were mixed with 2 mL scintillation fluid (Hionic-Fluor, Packard Bioscience, Groningen, Netherlands), and solubilized lipid was measured in a $\beta$-scintillation analyzer (Tri-Carb 1900 TR, Canberra Packard, Germany). 200 $\mu$L of a noncentrifuged bile salt/liposome mixture was used as the 100% value.

**Electron Microscopy.** All measurements were performed on a transmission electron microscope (LEO 912 Omega, Carl Zeiss, Oberkochen) using an acceleration voltage of 120 kV.

For visualization of inner structures, sections of the embedded material were investigated. Liposome dispersions were concentrated by ultracentrifugation (95 000 × g, 45 min). Pellets were transferred into silicon forms. Water-soluble melamine resin (nanoplast, Bachhuber, Ulm, Germany) was prepared according to the manufacturer's instructions. The resin was mixed with the liposome pellet and dried in an exsiccator for 48 h at room temperature, then for 24 h each at 40 °C and at 60 °C. From the hard resin block, ultrathin sections of 50−100 nm were prepared using a microtome (Ultracut E, Reichert & Jung, Leica, Vienna, Austria) at room temperature. The sections were transferred to copper grids (Science Services, Munich, Germany), positively stained by $RuO_4$, which was produced by oxidation of ruthenium(III) chloride (Merck, Darmstadt) with a 10% NaOCl solution (Sigma) in a closed staining chamber, and examined in the electron microscope.

## Results and Discussion

For the preparation of an inner liposomal polymer membrane skeleton, a weakly basic water-soluble monomer (DMAPMA) was tested for its suitability by determining the pH-dependent lipophilicity and insertion into a lipid monolayer. Liposomes containing a reactive membrane anchor (DOGM) were prepared by a detergent removal technique in order to encapsulate the hydrophilic monomer. Free DMAPMA was separated from the liposomes by centrifugation through a molecular sieve, and the release rate of the monomer from the vesicles was then measured

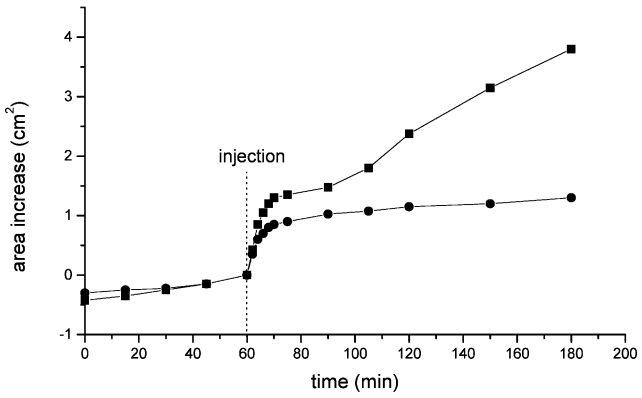


**Figure 2.** Interaction of the monomer DMAPMA with membrane lipids measured by increase of the phospholipid monolayer area. At equilibrium of the monolayer for 1 h in a Langmuir trough, the monomer was injected into the subphase, and the increase in area was measured at pH values below and above the monomer p$K_a$. ●, pH 6; ■, pH 10.

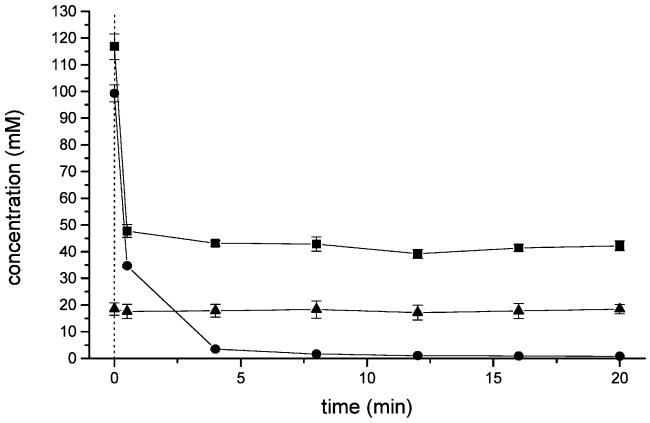


**Figure 3.** Sorption kinetics of dissolved compounds to Biobeads during liposome preparation by detergent removal from mixed micelles: ●, octyl glucoside (detergent); ▲, egg lecithin (membrane lipid); ■, DMAPMA (monomer).

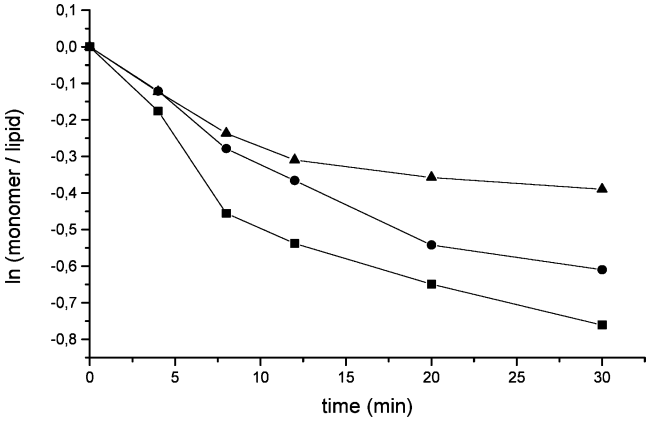


**Figure 4.** Kinetics of DMAPMA (monomer) release at different pHs from liposomes after separation from free monomer. Liposomally entrapped monomer was measured after separation of free monomer at different time points. At $t = 0$ min, the ratio of encapsulated monomer to membrane lipid was set as 100%. Membrane composition: egg lecithin/membrane anchor (DOGM) 98:2 (mol %). ▲, pH 6; ●, pH 9; ■, pH 10.

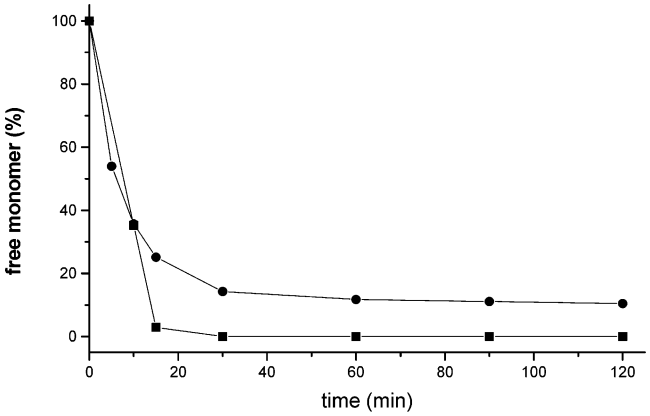


**Figure 5.** Kinetics of polymerization of DMAPMA in liposomes. Polymerization was followed at pH 9 (●) or pH 10 (■) by terminating the reaction at different time points with methoxyphenol. The remaining monomer concentration was determined with HPTLC.

to optimize the polymerization conditions of the membrane-skeleton liposomes (MSL). The structure of the polymer in the MSL was evaluated by electron microscopy, and the stability of the membrane against surfactant was quantified by the lowest concentration of sodium cholate required to solubilize the radioactively labeled membrane lecithin.

**Monomer Lipophilicity.** The p$K_a$ value of DMAPMA was determined to be 9.25, which is in agreement with the literature.[35] Above this value, the predominantly uncharged monomer should exert an increased lipophilicity as a prerequisite for the insertion into the lipophilic interior of the lipid membrane. Indeed, the measured octanol/water partition of DMAPMA was determined to be 0.004 at pH 6 and 3.2 at pH 10.

**Stability of the Monomer at Different pH.** A further prerequisite for the suitability of DMAPMA is its chemical stability at the high pH used. Quantification of the monomer in aqueous solution with HPTLC resulted in a decrease in monomer concentration after 30 min of approximately 1% at neutral pH and 7% at pH 10. This stability is sufficient for the applied liposome preparation and polymerization time.

**Monomer Interaction with Lipid Monolayer at Different pH.** The novel method of MSL synthesis should result in a shell-like hydrophilic polymer skeleton with a small distance to the inner liposomal membrane surface. This can be achieved by monomer adsorption to the membrane, followed by polymerization of the monomer and a pH-dependent desorption of the polymer network from the inner membrane surface. To get a better understanding of pH-dependent monomer adsorption, we used a lipid monolayer at the air/water interface of a Langmuir−Blodgett film balance. After equilibration of the lipid monolayer for 1 h, the monomer was injected into the subphase while maintaining constant film pressure. The adsorption of monomers to the lipid membrane results in an increase of the film area (initially 70 cm$^2$), as shown in Figure 2. The amount of inserted or adsorbed monomer is clearly dependent on the pH of the aqueous subphase. At pH 6, we observed a slight increase in film area, and after approximately 30 min, there is no further expansion of the film. On the other hand, at pH 10, an almost linear insertion rate for at least 2 h can be observed. This could be explained by a successive redistribution of monomer with increased lipophilicity from the aqueous into the lipidic phase. With the relatively small inner diameter of the liposomes of approximately 90 nm taken into account (see below), the redistribution process in the liposome interior should work on a much faster time scale than in the film balance subphase exhibiting a thickness of 3 mm.

**Liposome Preparation.** Unilamellarity of liposomes is crucial for their use as model membranes and the synthesis of a polymer to the inner membrane surface. The method of detergent removal is the most suitable procedure to yield predominantly unilamellar structures.[31] Furthermore, detergent

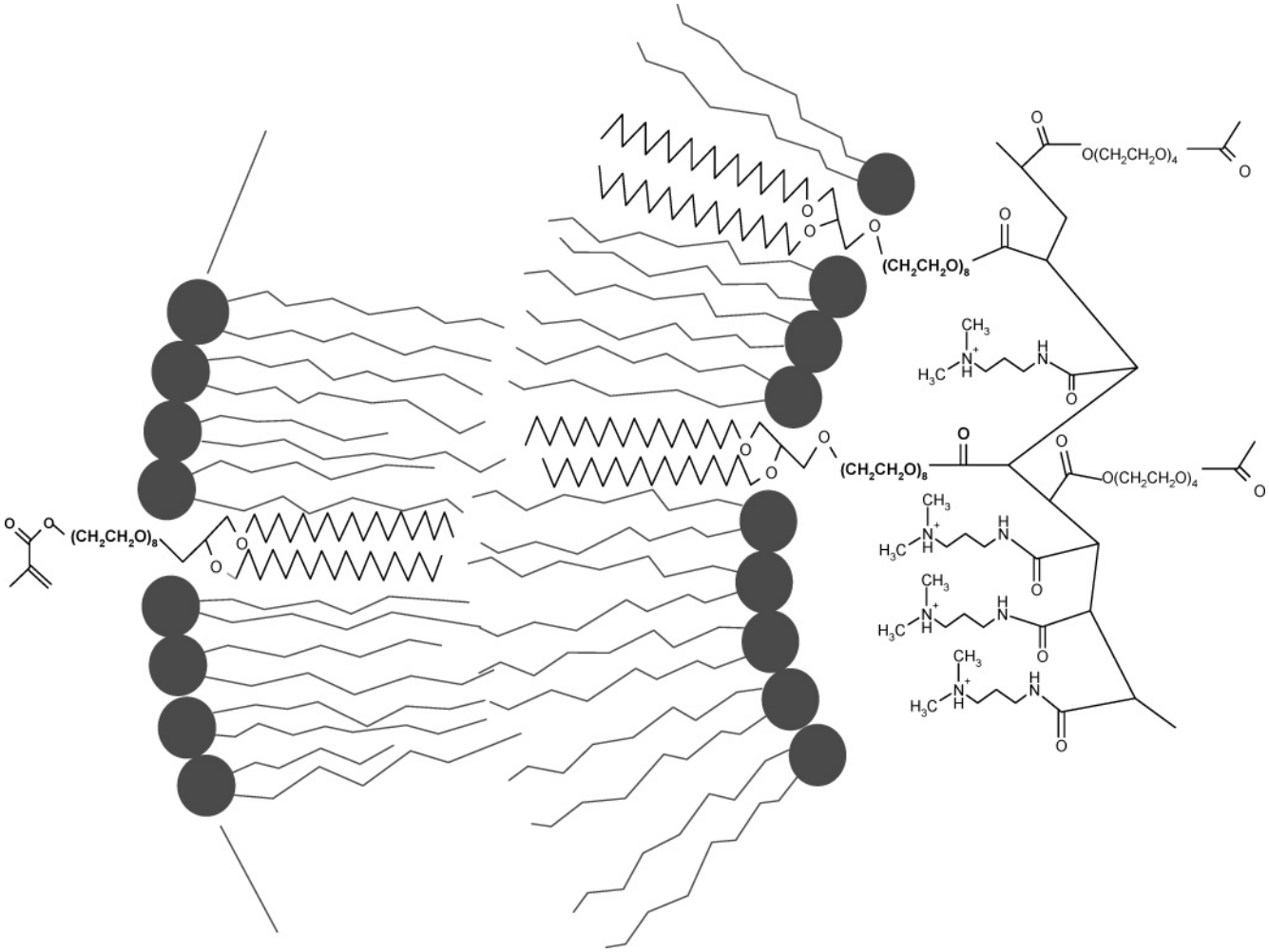

**Figure 6.** Schematic representation of the inner polymer membranes skeleton. The polymerizable membrane anchor DOGM is inserted into the inner and outer monolayer and is polymerized together with the monomer DMAPMA and the cross-linking TDGM almost exclusively at the inner membrane surface. The hydrophilic lamellar polymer skeleton has a distance to the membrane surface defined by the length of the oligooxyethylene spacer of the DOGM.

removal by using surfactant-adsorptive beads in particular ensures very fast liposome formation and avoids dilution of the lipid and the monomer. Therefore, this method was optimized for the lipid and monomer used. As shown in Figure 3, egg lecithin used as the membrane lipid is essentially not adsorbed to the beads, and the initial concentration of approximately 20 mM in the dispersion remains constant over the time of liposome preparation. A high portion of the water-soluble monomer DMAPMA is indeed removed by adsorption to the beads within less than 1 min. Thereafter, a constant concentration of around 45 mM in the aqueous phase is then achieved, which is high enough to form a polymer network within the liposome after polymerization. The initial removal of 100 mM OG is complete within 8 min. This coincides with the time required for the formation of liposomes, which were essentially unilamellar as evaluated by cryoelectron microscopy (not shown). Liposomes had a diameter of 100 nm (polydispersity index 0.15) as determined by photon correlation spectroscopy and by cryoelectron microscopy (100 nm, s.d. $\pm$ 35 nm; data not shown).

Prior to further experiments or polymer synthesis, nonencapsulated monomer was then removed completely by rapid centrifugation through a Sephadex G-50 column.

**Membrane Permeation.** As the permeation rate of the monomer correlates with its lipophilicity, the monomer release from liposomes after separation of non-encapsulated monomer should be faster at pH 10 compared to pH 6. This unwanted effect was substantiated by permeation measurements using a method of liposome centrifugation through the molecular sieve Sephadex G-50. Figure 4 shows a pronounced dependency of the permeation rate and the pH. Below the p$K_a$ at pH 6, an initial release rate with expected first-order kinetics decreases to end up in an almost stable encapsulation of the rest of the monomer after approximately 30 min. This late, hampered release may be a result of increasing membrane potential arising from losing charged monomer in the interior. At pH 9, which is very close to the p$K_a$ value, an increasing amount of uncharged monomer is able to leave the membrane vesicles. The release is even more pronounced at pH 10, above the p$K_a$ value. The nonlinearity in the semilogarithmic plot, i.e., deviation from first-order kinetics, in this case is probably due to the increased monomer portion adsorbed to the membrane surface. After approximately 20 min, half of the monomer is still encapsulated in the liposomes. At a lipid concentration of approximately 0.6 mM during polymerization and a liposome diameter of around 100 nm, the portion of the inner liposomal aqueous space compared to the total aqueous volume can be calculated[36] to be $<0.3\%$. Therefore, in the continuous outer phase, the released monomer and the forming polymer are additonally diluted to $>1{:}300$, and a polymerization time shorter than 30 min consequently leads to a polymer network which is almost entirely restricted to the inside of the liposome.

Kinetics of UV-Induced Polymerization. After fast removal of non-encapsulated DMAPMA, the polymerization kinetics

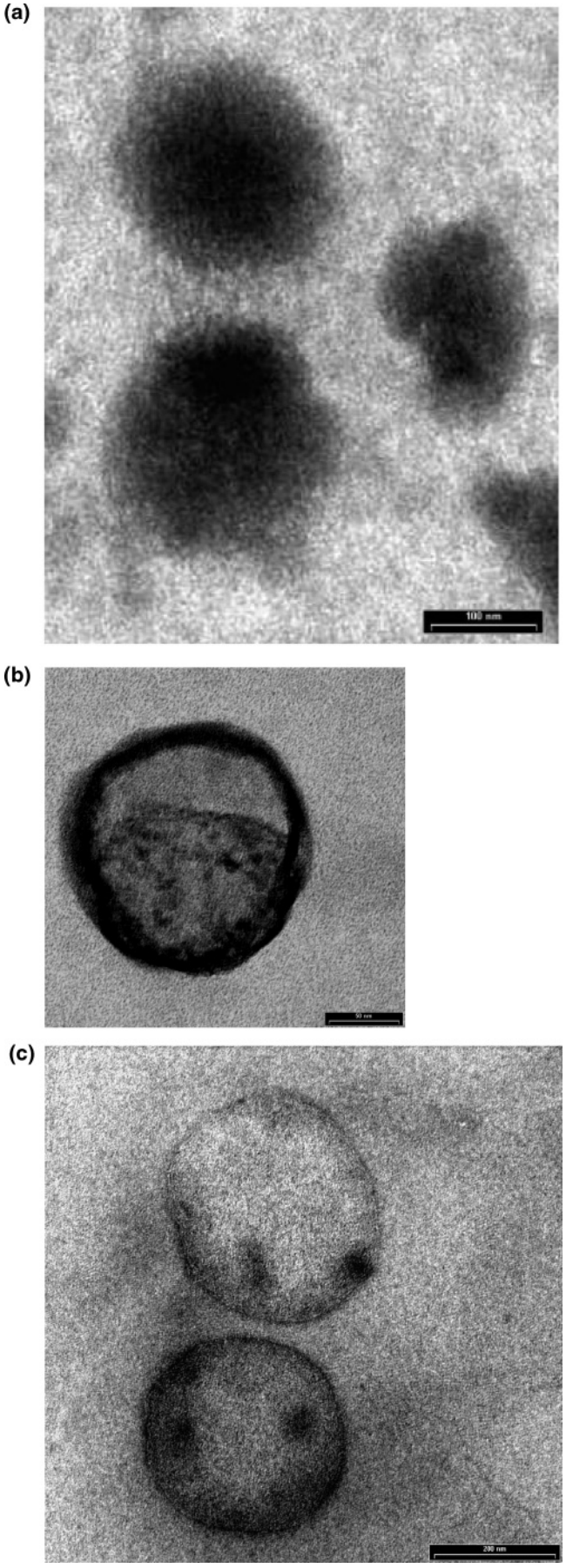


**Figure 7.** Transmission electron micrographs of ultrathin sections of liposomes with an inner polymer. Samples were negatively stained with $RuO_4$ vapor. Polymerization of DMAPMA (a) at pH 6; (b) and (c) at pH 10. Bars represent 100 nm in (a), 50 nm in (b), and 200 nm in (c).

were followed by the decrease in residual monomer. As shown in Figure 5, at an initial pH of 10, the monomer decreases to less than 3% within 15 min. This was therefore found to be the optimal polymerization time with regard to the kinetics of monomer release from the interior of the liposomes as shown above. Interestingly, at pH 9, just below the p$K_a$ value, polymerization was not complete even after 3 h. After a polymerization time of 15 min, the pH was close to 8.3, independent of the initial pH.

**Characterization of MSL.** The size of the membrane-skeleton liposomes was determined by photon correlation spectroscopy and cryo-EM to be approximately 100 nm (polydispersity index, 0.15). In comparison to the liposomes encapsulating the monomer before polymerization, no significant size alteration occurred through the polymerization process.

An optimal synthesis strategy should result in a polyDMAPMA cross-linked by TEGDM to form a hollow sphere-like structure and connected to the inner liposomal monolayer via the membrane anchor DOGM, as shown in Figure 6. The most suitable method to verify the resembled structure is electron microscopy. In cryo-EM pictures, the polymer structure could not be detected because of low contrast. However, staining of the polymer made its structure visible. As shown in the negative contrasted ultrathin sections shown in Figure 7a, polymerization at pH 6, where the monomer is charged and freely dissolved in the aqueous phase, resulted in a bulk polymer filling the entire inner space of the liposomes. However, when polymerization was performed after monomer adsorption to the inner liposomal monolayer at pH 10 (above the p*K* value), the polymer forms the desired hollow sphere structure within the liposomes, as can be seen in Figure 7b. In some preparations, smaller particulate polymer structures were found in the liposomes in addition to the clearly dark-stained polymer associated with the membrane (Figure 7c). After decreasing the pH to 6, the basic polymer is positively charged and should therefore be detached from the membrane surface. These pictures clearly show that the concept of adsorption of the monomer DMAPMA above the p$K_a$ value and desorption of the polymer below the p$K_a$ can successfully be realized.

**MSL Stability against Sodium Cholate.** Liposomes are solubilized by bile salts as natural detergents above a critical onset concentration, depending on the bile salt species and the lipid.[12,16] In a first step, mixed micelles of membrane lipid and bile salt molecules are then formed, which coexist with lamellar membrane remnants. At higher bile salt concentrations, the solubilization is complete and results exclusively in detergent/lipid mixed micelles. When an artificial membrane skeleton stabilizes the membrane against detergents, an increase of the onset concentration of solubilization should be found. Quantification of the membrane solubilization by determining the radioactively labeled membrane lipid in the supernatant after ultracentrifugation is shown in Figure 8. The onset of solubilization of polymer-stabilized liposomes occurs at approximately 13 mM sodium cholate, and the solubilization is complete at approximately 25 mM. As a control, the possible membrane stabilizing effect of 2 mol % of the membrane anchor DOGM in the egg lecithin membrane was also quantified. In this case, the onset of solubilization was found to be approximately 5 mM cholate, and solubilization was complete at 10 mM. This lower stability is essentially the same as when using pure egg lecithin liposomes.[12] The low amount of the rigid membrane anchor therefore does not contribute to membrane stabilization, whereas the artificial cytoskeleton restricted to the inner liposomal monolayer clearly stabilizes the membrane against the bile salt by a factor of approximately 2.5. In comparison to the membrane

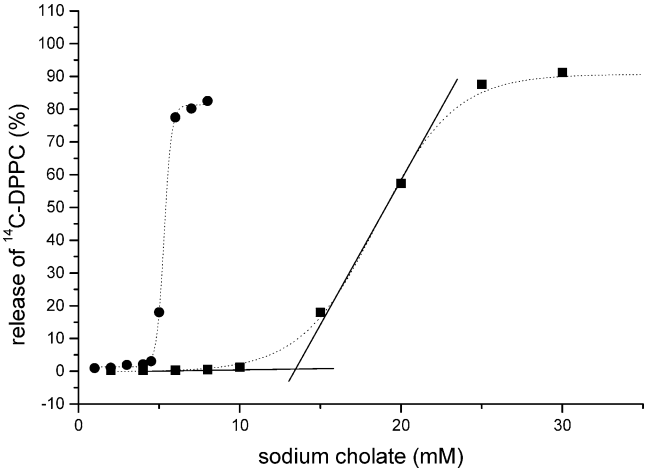


**Figure 8.** Solubilization of liposomal membranes with sodium cholate. Solubilization of membrane lipid was determined by measuring the release of $^{14}$C-labeled lecithin at increasing cholate concentration and separation of solubilized lipid from residual membranes by ultracentrifugation. ●, liposomes composed of egg lecithin/DOGM 98:2 mol %; ■, liposomes with the same lipid composition and an inner DMAPMA-based membrane skeleton.

skeleton formed by NIPAM, which causes a shift of the solubilization onset to approximately 8 mM cholate,[29] the stabilization by the DMAPMA skeleton is even more pronounced. As shown earlier,[16] solubilization of the membrane by bile salts is initiated by transient defect formation, when parts of the membrane lipids redistribute from the outer to the inner monolayer after bile salt attachment. In a second step, mixed micelles of lipids and bile salts are then released from the residual membrane bilayer. An inner polymer skeleton obviously blocks bilayer redistribution and/or the release of parts of the membranes. This stabilization may also be helpful, when membrane skeleton liposomes are designed to be used as drug carriers.

A potentially altered viscoelasticity of this type of liposome, the elucidation of which is part of our future studies, can also influence their recognition and uptake by cells of the immune system or by other target cells for drug delivery.

## Conclusion

The study presented here shows that a lamellar inner-membrane skeleton in liposomes mimicking the plasma membrane cytoskeleton of living cells can be synthesized by adsorption of a weak basic monomer such as DMAPMA to the inner membrane monolayer at elevated pH before polymerization. The chosen monomer has, in comparison to the NIPAM which was used in previous studies, the advantage of much slower membrane permeation and can therefore be restricted in the liposomal interior during the polymerization process. The consequences of this kind of artificial inner membrane skeleton on membrane properties such as viscoelasticity, lipid exchange, or lipid flip-flop are currently being investigated by AFM, micro-quartz balance, and electrophoretic methods.

The artificial membrane skeleton shows a remarkable membrane-stabilizing effect against the attack of bile salts. The structure of the polymer skeleton is comparable to the natural cytoskeleton in the plasma membrane of cells because of the formation of a similar planar network in the aqueous space, which is linked via hydrophilic spacers to membrane anchors at the inner membrane surface. Therefore, this finding may be helpful in the discussion of some aspects of membrane/bile salt interaction. In the liver, despite the high bile salt concentration of up to 40 mM,[17,18] the canalicular plasma membrane of the liver cells (cLPM) is stable against bile salts. The reason for this is still controversially discussed. One opinion is that sphingomyelin plays an important role in this stabilization process.[37] However, when using artificial membranes with a high sphingomyelin content, this concept has been shown to be questionable.[12] Our data presented here would support an essential contribution of the membrane-associated cytoskeleton for the stabilization of the cLMP.

**Acknowledgment.** The financial support of this study by the Sonderforschunsgbereich 428, Teilprojekt D4, is gratefully acknowledged. Authors thank Andreas Neub for performing the cryoelectron microscopic studies.

## References and Notes

(1) Sessa, G.; Weissmann, G. *J. Biol. Chem.* **1970**, *245*, 3295−3301.
(2) Medina, O. P.; Zhu, Y.; Kairemo, K. *Curr. Pharm. Des.* **2004**, *10*, 2981−9.
(3) Metselaar, J. M.; Mastrobattista, E.; Storm, G. *Med. Chem.* **2002**, *2*, 319−29.
(4) Leserman, L. J. *Liposome Res.* **2004**, *14*, 175−89.
(5) Derycke, A. S.; de Witte, P. A. *Adv. Drug Del. Rev.* **2004**, *56*, 17−30.
(6) Oberholzer, T.; Luisi, P. L. *J. Biol. Phys.* **2002**, *28*, 733−44.
(7) Harder, T.; van Meer, G. *Traffic* **2003**, *4*, 812−20.
(8) Bergstrand, N.; Arfvidsson, M. C.; Kim, J. M.; Thompson, D. H.; Edwards, K. *Biophys. Chem.* **2003**, *104*, 361−79.
(9) Bangham, A. D.; Standish, M. M.; Watkins, J. C. *J. Mol. Biol.* **1965**, *13*, 238−52.
(10) Bresseleers, G. J. M.; Goderis, H. L.; Tobback, P. P. *Biochim. Biophys. Acta* **1984**, *772*, 374−82.
(11) Deamer, D.; Bramhall, J. *Chem. Phys. Lipids* **1986**, *127*, 471−88.
(12) Schubert, R.; Beyer, K.; Wolburg, H.; Schmidt, K. H. *Biochemistry* **1986**, *25*, 5263−69.
(13) Hellwich, U.; Schubert, R. *Biochem. Pharmacol.* **1995**, *49*, 511−17.
(14) Sackmann, E. Biological membranes. Architecture and Function. In *Handbook of Biological Physics*; Lipowski, R., Sackmann, E., Eds.; Elsevier Science B. V.: Amsterdam, 1995; Vol. 1.
(15) Sackmann, E. Physical Basis of Self-Organization and Function of Membranes: Physics of Vesicles. In *Handbook of Biological Physics*; Lipowski, R., Sackmann, E., Eds.; Elsevier Science B. V.: Amsterdam, 1995; Vol. 1A.
(16) Schubert, R.; Schmidt, K. H. *Biochemistry* **1988**, *27*, 8787−94.
(17) Schiffman, M. L.; Sugerman, H. J.; Kellum, J. M.; Moore, E. W. *Gastroenterology* **1992**, *103*, 214−21.
(18) Klaassen, C. D.; Watkins, J. B. *Pharm. Rev.* **1984**, *36*, 1−67.
(19) Yeagle, P. *The Membranes of Cells*; Academic Press: Orlando, FL, 1987.
(20) Limozin, L.; Sackmann, E. *Phys. Rev. Lett.* **2002**, *89*, 168103.
(21) Regen, S. L.; Czech, B.; Singh, A. *J. Am. Chem. Soc.* **1980**, *102*, 6638−40.
(22) Hub, H.-H.; Hupfer, B.; Koch, H.; Ringsdorf, H. *Angew. Chem., Int. Ed.* **1980**, *19*, 938−40.
(23) Fendler, J. *Science* **1985**, *223*, 888−94.
(24) Chen, H.; Torchilin, V.; Langer, R. *J. Controlled Release* **1996**, *42*, 263−72.
(25) Ringsdorf, H.; Sackmann, E.; Simon, J.; Winnik, F. M. *Biochim. Biophys. Acta* **1993**, *1153*, 335−44.
(26) Kono, K.; Nakai, R.; Morimoto, K.; Takagishi, T. *Biochim. Biophys. Acta* **1999**, *1416*, 239−50.
(27) Yamazaki, A.; Winnik, F. M.; Cornelius, R. M.; Brash, J. L. *Biochim. Biophys. Acta* **1999**, *1421*, 103−15.
(28) Hotz, J.; Meier, W. *Langmuir* **1998**, *14*, 1031−6.
(29) Stauch, O.; Uhlmann, T.; Fröhlich, M.; Thomann, R.; El-Badry, M.; Kim, Y.-K.; Schubert, R. *Biomacromolecules* **2002**, *3*, 324−32.
(30) Stauch, O.; Schubert, R.; Savin, G.; Burchard, W. *Biomacromolecules* **2002**, *3*, 565−78.
(31) Schubert, R. *Methods Enzymol.* **2003**, *367*, 46−70.
(32) Philippot, J. R. *Biochim. Biophys. Acta* **1985**, *821*, 79−84.
(33) Holloway, P. W. *Anal. Biochem.* **1973**, *53*, 304−8.
(34) Bartlett, G. R. *J. Biol. Chem.* **1959**, *234*, 466−8.
(35) Kazentsev, O. A.; Shirshin, K. V.; Kazakov, S. A.; Danov, S. M. *Russ. J. Gen. Chem.* **1996**, *66*, 1958−62.
(36) Schubert, R.; Wolburg, H.; Schmidt, K. H.; Roth H. J. *Chem. Phys. Lipids* **1991**, *58*, 121−9.
(37) Gerloff, T.; Meier, P. J.; Stieger, B. *Liver* **1998**, *18*, 306−12.

BM0580126